ELSEVIER

International Journal of Heat and Fluid Flow 19 (1998) 167–172

International Journal of
HEAT AND
FLUID FLOW

Heat up and evaporation of shear driven liquid wall films in hot turbulent air flow

Heiko Rosskamp, Michael Willmann, Sigmar Wittig *

Institut für Thermische Strömungsmaschinen, University of Karlsruhe, Kaiserstrasse 12, 76131 Karlsruhe, Germany

Received 15 July 1997; accepted 25 October 1997

Abstract

Evaporating shear driven liquid wall films play an important role in the fuel preparation process of advanced gas turbine combustion chambers. In extending earlier studies of Sill, K.H., 1980. Sammelband der VGB-Tagung, May 1980, pp. 232–238 and Himmelsbach, J., Noll, B., Wittig, S., 1994. Int. Journal of Heat and Mass Transfer 37, 1217–1226, the present analysis of shear driven liquid films in a rectangular model duct is directed into the boundary layer flow at the gas-liquid interface and the wall film itself. The experimental conditions range from 314 to 373 K at atmospheric pressure giving duct flow Reynolds numbers of 81 000–162 000. The liquid mass flux for the film is varied between 33.3 g/sm and 100 g/sm. The experimental analysis includes spatially resolved measurements of interfacial shear stress, gas phase velocity and temperature profiles as well as the wall conditions. The film itself is investigated regarding its thickness and evaporation behaviour. Finally, a reference data set for comparison with CFD-data is obtained. The results obtained suggest that the theoretical models which are currently in use should be modified with regard to the interfacial shear stress development in the axial direction.

Keywords: Shear driven wall film; Liquid film; Interfacial shear stress; Turbulent boundary layer

1. Introduction

Careful fuel preparation is a key issue in modern combustors to achieve low NO_x emissions. This may be accomplished by premix ducts or advanced prefilming atomizers. In these devices shear driven liquid wall films play an important role. Fuel evaporation and fuel coking are closely related to the flow characteristics and heat up of the liquid film. A number of studies have covered this topic in the past (Sill, 1980; Kuck, 1982; Pfeiffer et al., 1991; Wittig et al., 1991). However, in these studies, the film was either considered as a side effect or the investigations focused largely on the film itself. There is still a lack of investigations that account for the strongly coupled behaviour of gas and film flow. Recent advances in the two-phase flow computation of combustor flows (Kurreck et al., 1996; Rosskamp et al., 1997) demand improved models that describe evaporating fuel films. This in turn requires a more profound understanding of the two-phase flow behaviour and a detailed database as a reference.

Currently, the film flow is considered to be laminar in the computer codes developed. The state of the interface is assumed to be represented either by a smooth surface (Baumann et al., 1989) or, in the more advanced models, as a rough wall (Himmelsbach et al., 1994; Rosskamp et al., 1997) (Fig. 1(b)). In either case, the velocity of this virtual "wall" has been neglected so far. Very detailed work on the internal velocity profile of thin shear driven films at ambient conditions has been recently presented by Wittig et al. (1996) and Samenfink et al. (1996) providing a better basis for modeling of the wall film flow itself. The roll waves occur randomly and are rather different in size and shape. However, statistically the wave flow can be contemplated as indicated in Fig. 1(b). As the waves travel typically with a velocity which is approximately two orders of magnitude smaller than the gas velocity, the gas/film interface is considered as a very slow moving or non-moving rough wall. Due to this roughness and due to blowing by evaporation, the film heavily affects the gas phase boundary layer. Fig. 1(b) presents a sketch of the gas phase boundary layer, the interface and the film flow. The flow characteristics of films on smooth surfaces are exclusively affected by the wall heat transfer, the interfacial shear stress and the interfacial heat transfer which in turn can be traced back to the shear stress. Therefore, it is of particular importance to relate properties such as the film thickness and film roughness for example to the interfacial shear stress. This often is not accounted for in the literature. Only Sill (1982) has investigated both the film flow *and* the boundary layer in some detail. However, a complete view and a reference data base of the two-phase flow are still missing.

Therefore, the present study focuses on the heat up and evaporation of a shear driven model wall film interacting with a turbulent boundary layer to give an improved experimental background for modeling. A second aim is to provide a reference data set for a selected flow case with measurements taken

* Corresponding author. E-mail: wittig@itsnova.mach.uni-karslruhe.de.

0142-727X/98/$19.00
PII: S0142-727X(97)10021-2

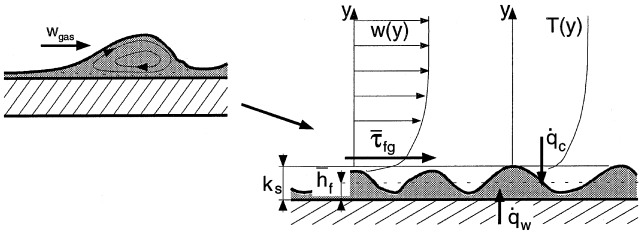

Fig. 1. (a) Roll wave of shear driven film, (b) wall film and gas boundary layer.

over the length of the film including starting conditions and turbulence characteristics of the gas flow.

2. Test rig

For the experiments, a hot gas test facility at the Institut für Thermische Strömungsmaschinen is used. A blower delivers an air mass flux up to $\dot{m}_{\text{air}} = 0.6$ kg/s which is heated up to $T = 500$ K in a 90 kW electrical heater. A surge tank and a 1.2 m long inlet section with turbulence grids guarantee evenly developed turbulent flow at the inlet of the test section. Fig. 2 presents a longitudinal section of the test section. The cross section of each channel half is $\Delta x = 0.1$ m wide and $\Delta y = 0.055$ m high. Between the two channel halves, the prefilming plate is mounted.

In the middle of the prefilming plate there is a roughened 50 mm wide cavity which is 200 μm deep to guarantee a well-defined film width. The prefilming plate is insulated in the transverse direction to avoid any three-dimensional heat fluxes in the prefilming plate and the film itself. Fig. 3 shows an enlarged view of the prefilmer and the cavity. At the inclined outlet of the prefilmer, the film is still rather smooth and the average film thickness corresponds almost to the cavity depth. This design avoids a strong discontinuity in surface roughness at the prefilmer enabling more precise boundary layer measurements close to the film inlet. Water serves as test fluid for the experiments presented here.

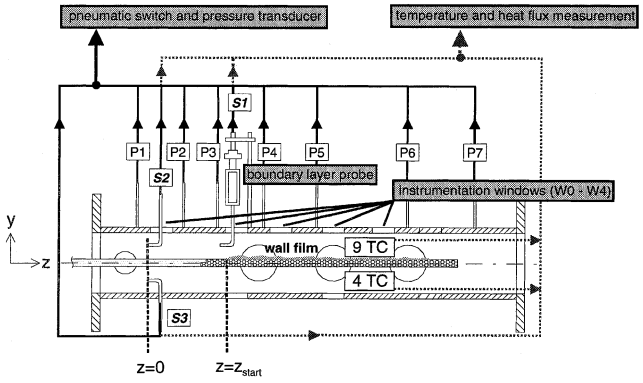

Fig. 2. Sketch of wall film test section (TC = thermo-couples).

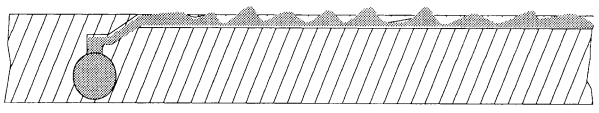

Fig. 3. Longitudinal section of prefilmer and cavity.

Table 1
Measurement locations

z_{position} (m)	$W0$	$W1$	$W2$	$W3$	$W4$		
w-, T-profiles	0.000	0.168	0.267	0.377	0.487		
Film thickness	–	0.181	–	0.390	0.500		
	$P1$	$P2$	$P3$	$P4$	$P5$	$P6$	$P7$
Static pressure	−0.026	0.076	0.134	0.224	0.375	0.554	0.686

All measurements are taken in the mid section of the duct presupposing flow two-dimensionality. The measurement locations are referenced in Table 1. All measures refer to z_0 as indicated in Fig. 2. The film starts at $z_{\text{start}} = 0.155$ m.

3. Measurement techniques and data processing

Test rig control and data monitoring are accomplished by means of a PC-based system. Wall heat flux is measured with the temperature gradient method. Due to thermocouple measurement errors and uncertainties in mounting, this method has an uncertainty in heat flux measurements of about 7% for the 373 K measurements. The turbulence characteristics of the plain air flow are measured using a single wire DANTEC hot wire device. In order to cover the whole turbulent regime, data are sampled to 50 kHz. The integral length scale is determined from the power spectrum using the Taylor hypothesis:

$$I_X = \left(\frac{E(f)\overline{w}}{4 w_{\text{RMS}}} \right)_{f \to 0}, \tag{1}$$

$$L_x = \overline{w} l_x. \tag{2}$$

The hot-wire data fit the von Karman spectrum quite well indicating isotropic turbulence.

The interfacial shear stress is calculated according to the method of Ellis et al. (1959). The velocity measurements required for this method are taken with conventional pitot probe technique since the presence of a wall film and secondary droplets make the use of hot-wire probes prohibitive. To avoid errors in the measured velocity, the measurements in the boundary layer are corrected according to McMillan (1957) and Wuest (1969). For the calculation of the shear stress, the von Karman constant must be known. Detailed investigations of Pimenta et al. (1978) indicate that a constant value of κ may be used even in boundary layers on rough walls with blowing. If a liquid wall film is present, the temperature gradient between the free flow and the interface is very high leading to steep variations in fluid properties in the boundary layers. This is accounted for by an approach of Rüd (1985) that introduces reference properties at interface temperature and gives corrected values for the parameters of the logarithmic law of the wall. Additionally, the displacement thickness of the wall film is considered in the calculation of the non-dimensionalized wall coordinate.

Evaporation of the film fluid is measured in terms of a global evaporation rate according to

$$ev = \frac{\dot{m}^*_{f,\text{in}} - \dot{m}_{f,\text{out}}}{\dot{m}_{f,\text{in}}} \times 100\%. \tag{3}$$

The sucked mass flux at the end of the prefilming plate is compensated for the moisture that is sucked off together with the liquid and for the vapor loss in the vacuum suction bottle. In (3), $\dot{m}^*_f$ is the liquid mass flux per unit width. Evaporation is measured only for 33.3 g/sm and 50 g/sm due to limitations in the suction arrangement.

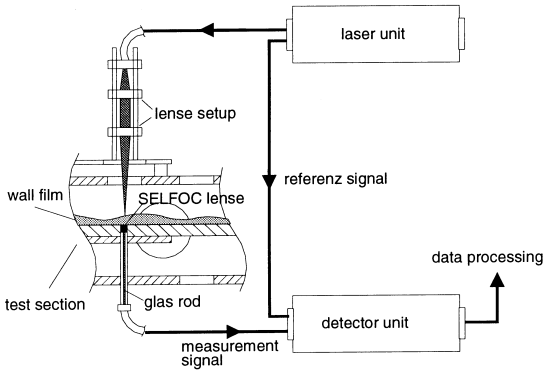

Fig. 4. Measurement of local film thickness.

The local film thickness is measured with a laser light absorption device (Sill, 1980; Wittig et al., 1991) (Fig. 4) to avoid any disturbance of the film flow. This technique is compatible with any fluid that has a high absorption coefficient in the infrared spectrum. A red and an infrared laser beam are superimposed and transmit the film. The infrared light is absorbed whereas the visible light experiences solely inter-phase scattering. By measuring the light intensities of the beam before and after it has passed the film, the film thickness can be calculated according to the law of Lambert–Beer:

$$h_f = -\frac{1}{k'} \ln \frac{I}{I_0}, \tag{4}$$

where I is the measured intensity, I_0 the reference intensity and k' the absorption constant of the fluid. The precision of the device is better than 7% at the same axial location.

4. Results

4.1. Plain air flow

The turbulence grids at the duct inlet provide an almost rectangular velocity profile that develops to a proper turbulent velocity profile in the actual test section. Fig. 5 presents the mean velocity profiles at Re = 162,000 (314 K). Due to boundary layer growth at the walls and their displacement effect, the free-stream velocity increases from 50 to 51.9 m/s. The flow is fully symmetric except at the outlet plane which is influenced by a reduction pipe in the exhaust. Also, the velocity profile in the transverse direction and the temperature profiles are carefully checked and found to be smooth. Therefore, velocity and temperature profiles are presented up to half the duct height in the following.

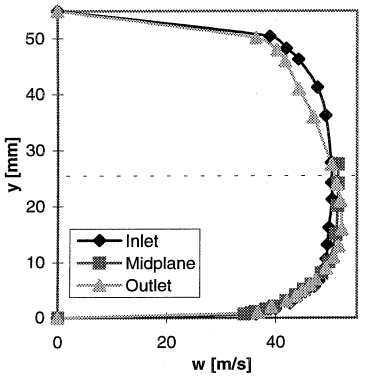

Fig. 5. Mean velocity profiles at Re = 162000 (314 K).

The conditions of plane $W0$ are taken as inlet conditions. All experiments presented here are conducted with an inlet velocity of $w = 50 \pm 0.2$ m/s. The free-stream turbulence is 2.3% (±0.1)% with an integral length scale of 5.4 mm (±0.4 mm). Under heated conditions, the flow structure remains rather unchanged as shown by Fig. 6. At 373 K, the turbulence level is little above 3% and also the integral length scale does not significantly change compared to the cold flow case.

Without any film, the plate acts as an almost isothermal boundary. Even though the cavity ground is sandblasted ($R_{z,\mathrm{DIN}} = 4.16$ μm), it appears hydraulically smooth. Therefore, the boundary layer development is rather similar to that of a flat plate. Boundary layer growth over the duct length leads to a velocity increase of 3% in the mid-section. No significant changes occur between the different temperature levels as indicated by the flow profiles in Fig. 6 and the shape factor H_{12} in Fig. 7. Fig. 7 and Fig. 8 present the axial development of the displacement thickness δ_1, momentum thickness δ_2 and interfacial shear stress τ for $T = 314$ K. The shear stress decreases only slightly as the boundary layer becomes thicker indicating that the boundary layer development is partly compensated by the minor increase in free-stream velocity. The superelevation in the shear stress curves at $z = 0.168$ m is attributed to the prefilmer 13 mm upstream this measurement location. If no film is supplied, the prefilmer appears at backward facing step of 0.2 mm height. Hence, the flow probably does not follow the logarithmic law exactly at $W1$, leading to slightly biased shear stress values in this case. Fig. 8 illustrates

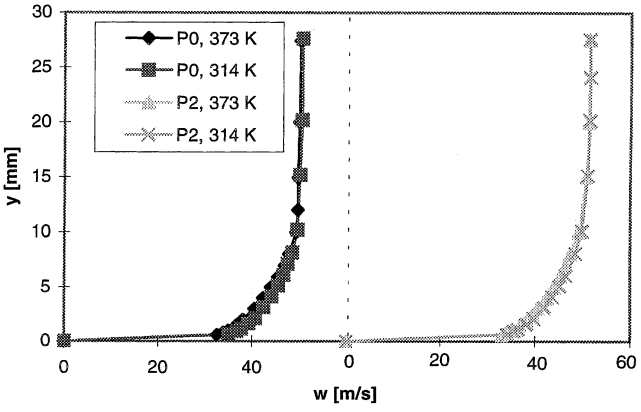

Fig. 6. Velocity profiles for cold and heated flow conditions.

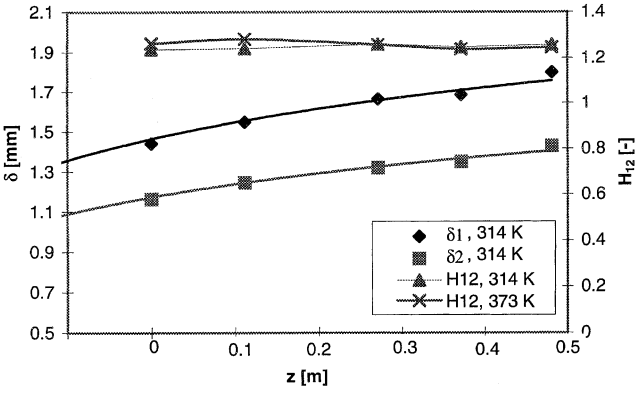

Fig. 7. Displacement thickness and momentum thickness at 314 K, shape factor at 314 K and 373 K.

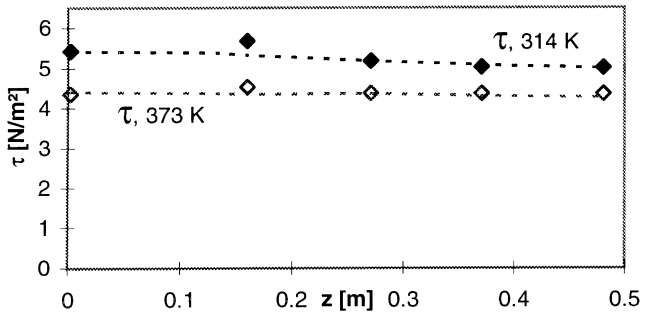

Fig. 8. Wall shear stress and wall temperature versus duct length.

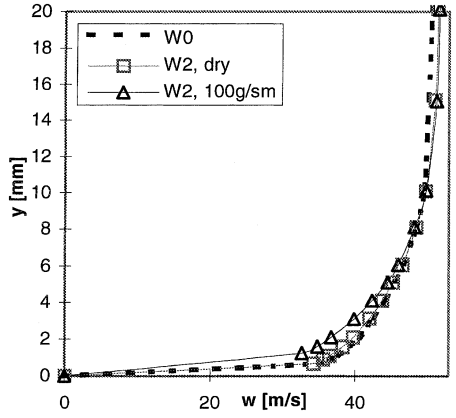

Fig. 9. Velocity profiles above smooth wall and liquid film, 314 K.

the effect of increased temperature. Due to reduced gas density, the shear stress is generally lower.

4.2. Cold two-phase flow

If a liquid wall film is present, the boundary layer is significantly affected by increased momentum and heat transfer. The effect of mass transfer can be neglected in this case as evaporation of the film (water, 100 g/sm) is very low. A displacement effect from the film on the gas phase is negligible. Fig. 9 shows the velocity profile over the film at plane 2 (*W*2, 100 g/sm) in comparison to the inlet profile (*W*0) and the dry case (*W*2, dry). The change in the velocity profile originates mainly from the increased roughness of the interface and, to a minor extent, from increased heat transfer. The interfacial shear stress increases by a factor of about 2.5 (Fig. 10). It rises rather slowly after the film inlet. The interfacial shear stress reaches its maximum right after plane 2 and settles further downstream. Visualization indicates that the film is almost smooth up to 10 mm downstream the prefilmer before the development of the typical roll wave pattern starts. For that reason, the interfacial shear stress at plane 1 (13 mm downstream of the prefilmer) has still not reached its maximum value for fully developed wavy film flow. The strong increase in momentum transfer is mirrored by a pronounced rise in momentum thickness shown in Fig. 10. Also, the shape factor becomes higher which is in good agreement with the results of Sill (1982).

Under these conditions, the film is about 147 μm thick at position *W*1 (Fig. 11). At plane 3 where the shear stress has already increased to its final value, the film thickness decreases to 124 μm. In addition, Fig. 11 illustrates the effect of a variation in liquid loading. As the mass flux increases, the mean film thickness rises degressively. This agrees well with the experimental findings of Wittig et al. (1991).

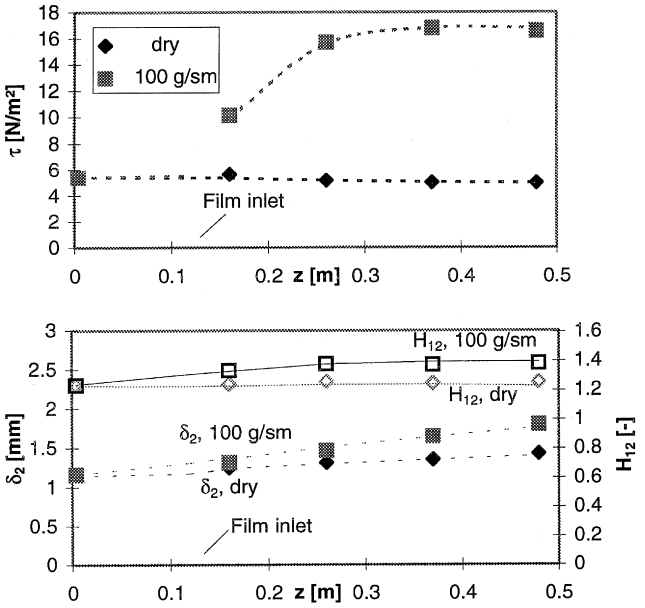

Fig. 10. Shear stress (top), momentum thickness, and shape factor (bottom) for dry and wetted wall.

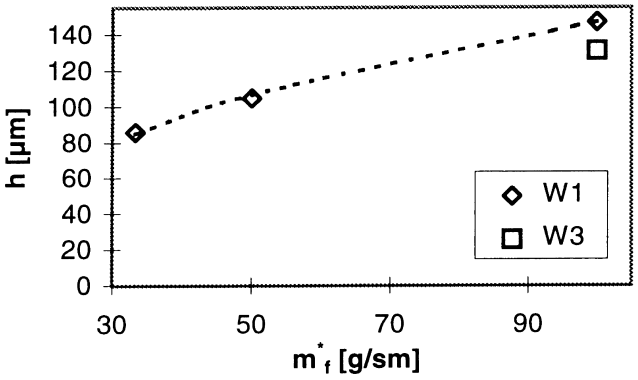

Fig. 11. Mean film thickness, 314 K.

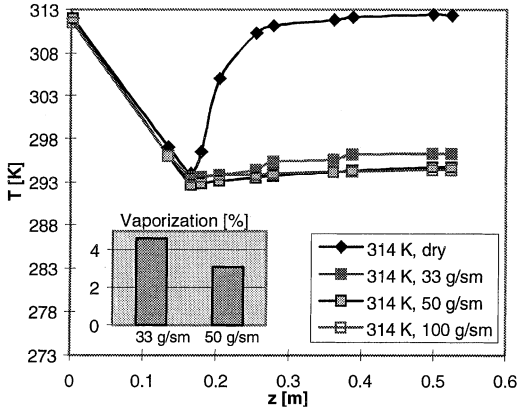

Fig. 12. Wall temperatures of prefilming plate and evaporation rates, 314 K.

Vaporization is rather low under cold conditions as shown in Fig. 12. The evaporation rate at 33 g/sm is almost twice as high as at 50 g/sm. This results from a much weaker film

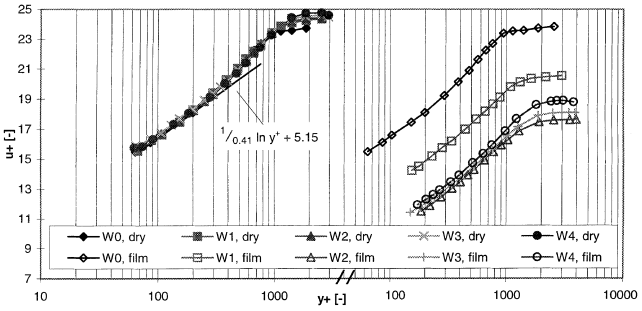

Fig. 13. Velocity profiles in non-dimensionalized form, dry and film 100 g/sm.

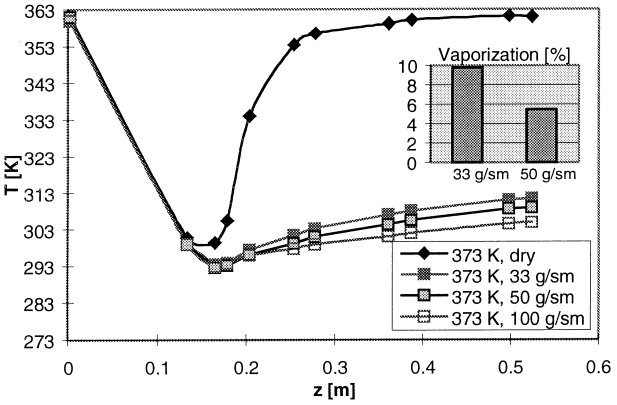

Fig. 15. Wall temperatures of prefilming plate and evaporation rates, 373 K.

heating which in turn depends strongly on the film thickness. The thicker films remain relatively cool due to their high heat capacity.

4.3. Hot two-phase flow

Under hot gas conditions, the velocity profiles generally develop analogously to the cold flow case (Figs. 9 and 10). Fig. 13 mirrors this behaviour in logarithmic representation.

The curves for dry flow coincide very well as shown on the left. The w^+-plot for the boundary layer over the film reveals the development of the film roughness. As the interface roughness increases the curves are shifted downwards. Again, the curves of the last three positions almost coincide indicating developed film flow from plane 2 onwards. This results in a shear stress evolution as shown in Fig. 14. The shear stress rises to a maximum at plane 2 in analogy to the cold flow case. However, the shear stress decreases slightly with the 373 K flow case. This may be explained by the strong heating of the film as shown in Fig. 15. This heating that is accompanied by a change in fluid properties evidently leads to a reduced interface roughness. By comparing the three curves $W2$, 3, 4 with film in Fig. 13 that almost collapse, it can be seen that curve $W4$ and $W3$ are slightly shifted upwards relative to curve $W2$. This reveals the change in interface roughness as discussed above. Analogous to the cold flow, the slow rise in the shear stress curve (Fig. 14) indicates that the interfacial roughness effect which is exerted by the liquid wall film develops rather smoothly at the film inlet. The slight decrease in shear stress downstream of plane 2 is solely attributed to a change in fluid properties because evaporation rates at 100 g/sm are too low to affect the mean film thickness significantly.

Evaporation rates with 33.3 and 50 g/sm are significantly higher than compared to the cold flow. This results from a considerably stronger heating of the film (Fig. 15).

The boundary layer characteristics do not significantly change compared to 314 K as indicated by Fig. 14. The momentum thickness rises more strongly with the film than without it. The shape factors remain almost the same compared to the cold flow.

5. Summary and conclusions

The shear driven wall film flow and the turbulent boundary layer above the film have been investigated in a rectangular model vaporizer duct. It is found that the turbulent boundary layer above a shear driven wall film behaves qualitatively similarly to a boundary layer on a dry surface. The increased interface roughness is reflected in an increased displacement thickness and momentum thickness. However, the shape factors rise only slightly compared to the dry flow. Measurements of the interfacial shear stress at the film surface show a rather smooth rise in the flow direction. Generally, the shear stress reaches a maximum at about 110 mm downstream the film inlet before leveling to a constant value (314 K) or slightly decreasing (373 K), respectively. This indicates that the typical surface pattern of the film develops comparably slowly leading first to a rising and afterwards to a slightly decreasing effective interface roughness. This phenomenon is clearly mirrored by the non-dimensionalized velocity plot. As evaporation rates are generally low in the experiments presented here, the decrease in roughness downstream of plane 2 is attributed to a change in fluid viscosity and surface tension due to increased temperatures. If the wall film flow has properly developed, the film thickness varies inversely with shear stress.

The results obtained suggest modifications to existing theoretical models for film flows in that a starting length for the film flow in terms of reduced film roughness should be introduced. With the detailed data set obtained in this work, a reference is provided that can serve for testing new CFD wall film models.

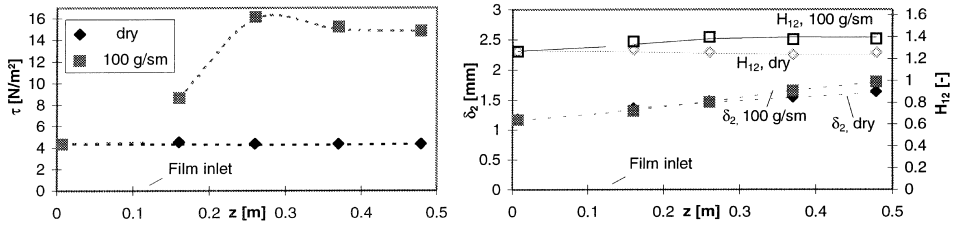

Fig. 14. Interfacial shear stress (left), momentum thickness and shape factor (right) for dry and wet conditions, 373 K.

6. Tabulated data

Tabulated data for the 314 K flow case with film (100 g/sm) are available upon request. The data comprise velocity and temperature data for the gas flow, pressure drop measurements, wall temperatures and heat fluxes as well as film thickness measurements.

For a copy of the data set please contact the authors.

Acknowledgements

This work was supported by a grant from the Graduiertenkolleg "Energie- und Umwelttechnik" through the Deutsche Forschungsgemeinschaft (DFG) which is gratefully acknowledged.

References

Baumann, W.W., Bendisch, H.H., Eickhoff, H., Thiele, F., 1989. Interaction of hot swirling air and liquid film flow in air blast atomizers. International Symposium on Air Breathing Engines, pp. 971–976.

Ellis, S.R., Gay, B., 1959. The parallel flow of two fluid streams: Interfacial shear stress and fluid-fluid interaction. Trans. Inst. Chem. Engrg. 37, 206–215.

Himmelsbach, J., Noll, B., Wittig, S., 1994. Experimental and numerical studies of evaporating wavy fuel films in turbulent air flow. Internat. J. Heat and Mass Transfer 37, 1217–1226.

Kuck, A., 1982. Experimentelle und theoretische Untersuchung der Vorgänge in einer zylindrischen Modellbrennkammer bei Wandauftragung des Kraftstoffs. Doctor thesis RWTH Aachen.

Kurreck, M., Willmann, M., Wittig, S., 1996. Prediction of the three-dimensional reacting two-phase flow within a jet-stabilized combustor. ASME Paper 96-GT-468.

McMillan, F.A., 1957. Experiments on pitot-tubes in shear flows. Great Britain ARC Report and Membership 3028, London.

Pfeiffer, A., Schulz, A., Wittig, S., 1991. Design and development of the ITS ceramic research combustor, Yokohama International Gas Turbine Congress, October 27th–November 1st 1991, Yokohama, Japan.

Pimenta, M.M., Moffat, R.J., Kays, W.M., 1978. The structure of a boundary layer on a rough wall with blowing and heat transfer, ASME Paper 78-HT-3.

Rosskamp, H., Willmann, M., Wittig, S., 1997. Computation of two-phase flows in low-NO_x combustor premix ducts utilizing fuel film evaporation. ASME Paper 97-GT-226.

Rüd, K., 1985. Transitionale Grenzschichten unter dem Einfluß hoher Freistromturbulenz, intensiver Wandkühlung und starker Druckgradienten in Heißgasströmungen. Doctor Thesis, University of Karlsruhe.

Rüd, K., Wittig, S., 1986. Laminar and transitional boundary layer structures in accelerating flow with heat transfer. ASME Paper 86-GT-97.

Samenfink, W., Elsäßer, Wittig, S., Dullenkopf, K., 1996. Internal transport mechanisms of shear-driven liquid films. Eighth International Symposium on Application of Laser Techniques to Fluid Mechanics, 6–11 July 1996, Lisbon, Portugal.

Sill, K.H., 1980. Experimentelle Bestimmung der Grenzflächenstruktur und der mittleren Filmdicke von strömenden Flüssigkeitsfilmen mit Hilfe der Lichtabsorptionsmethode. Forschung in der Kraftwerkstechnik 1980. Sammelband der VGB-Tagung. pp. 232–238.

Sill, K.H., 1982. Wärme- und Stoffübertragung in turbulenten Strömungsgrenzschichten längs verdunstender welliger Flüssigkeitsfilme. Doctor Thesis. University of Karlsruhe.

Wittig, S., Elsäßer, A., Samenfink, W., Ebner J., Dullenkopf, K., 1996. Velocity profiles in shear-driven liquid films: LDV-measurements, Eighth International Symposium on Applications of Laser Techniques of Fluid Mechanics, 6–11 July 1996, Lisbon, Portugal.

Wittig, S., Himmelsbach, J., Noll, B., Feld, H.-J., Samenfink, W., 1991. Motion and evaporation of shear-driven liquid films in turbulent gases. ASME-Paper 91-GT-207.

Wuest, W., 1969. Strömungsmeßtechnik. Vieweg.